Send Orders for Reprints to reprints@benthamscience.net

Current Enzyme Inhibition, xxxx, *xx*, 00-00

RESEARCH ARTICLE

Ovine COX-1 Isoenzyme Bio-production

Morena Miciaccia[1], Mariaclara Iaselli[1], Savina Ferorelli[1], Paola Loguercio Polosa[2], Maria Grazia Perrone[1,*] and Antonio Scilimati[1,*]

[1]*Department of Pharmacy – Pharmaceutical Sciences, University of Bari, Via E. Orabona 4, 70125 Bari, Italy;* [2]*Department of Biosciences, Biotechnologies, and Biopharmaceutics, University of Bari, Via E. Orabona 4, 70125 Bari, Italy*

ARTICLE HISTORY

Received: June 21, 2021
Revised: August 01, 2021
Accepted: September 24, 2021

DOI:
10.2174/1573408017666211108104731

Abstract: ***Background*:** Recent findings enlightened the pivotal role of cyclooxygenases-1 and -2 (COX-1 and COX-2) in human diseases with inflammation as the committed earliest stage, such as cancer and neurodegenerative diseases. COXs are the main targets of nonsteroidal anti-inflammatory drugs and catalyze the bis-oxygenation of arachidonic acid into prostaglandin PGH_2, then converted into prostaglandins, thromboxane, and prostacyclin by tissue-specific isomerases. A remarkable amount of pure COX-1 is necessary to investigate COX-1 structure and function, as well as for *in vitro* disease biochemical pathway investigations.

***Methods*:** *Spodoptera frugiperda* cells were infected with Baculovirus that revealed to be an efficient expression system to obtain a high amount of *ovine*(o)COX-1. Protein solubilization time in the presence of a non-ionic detergent was modified, and a second purification step was introduced.

***Results and Discussion*:** An improvement of a previously reported method for pure recombinant *o*COX-1 production and isolation has been achieved, leading to a lower starting volume of infected cells for each purification, an increased cell density, an increased number of viral particles per cell, and a shortened infection period. The protocol for the recombinant *o*COX-1 expression and purification has been in-depth elaborated to obtain 1 mg/L of protein.

***Conclusion*:** The optimized procedure could be suitable for producing other membrane proteins as well, for which an improvement in the solubilization step is necessary to have the availability of high concentration proteins.

Keywords: Cyclooxygenase (COX)-1, recombinant *ovine*COX-1, protein expression and purification, baculovirus, viral vector, Sf9 insect cells, non-steroidal anti-inflammatory drugs.

1. INTRODUCTION

Prostaglandin endoperoxide H synthase-1 and -2 (PGHS-1 and PGHS-2), also known as cyclooxygenases (COXs), are bifunctional, membrane-bound, and heme-containing enzymes. They catalyze the conversion of arachidonic acid (AA) into prostaglandin H_2 (PGH_2) as the committed step of prostanoid biosynthesis [1]. Both isoforms (COX-1 and COX-2) are homodimers with ~72 kDa monomer molecular mass [2-4].

COX isoenzymes expression is either constitutive or inducible, depending on the organ and specific physiopathological conditions. COX-2 is constitutively expressed in a limited number of tissues, in particular, brain and kidney; whereas, in almost all body districts, it is induced in response to inflammatory stimuli and growth factors upon a variety of pathological conditions, in which the inflammation is the earliest stage [5-7]. Various chemical mediators from the circulation system, inflammatory cells, and injured tissue contribute to affect the inflammatory response through vasoactive amines (histamine and serotonin), peptide (*e.g.*, bradykinin), and eicosanoids (*e.g.*, thromboxane, leukotrienes, and prostaglandins) [8, 9].

COX-1, differently from COX-2, is constitutively expressed in most tissues; it catalyzes the synthesis of prostaglandins responsible for maintaining homeostasis in some human body districts such as the cardiovascular system and gastric mucosa [10]. COX-1 is expressed at high levels, rather than COX-2, in the early to advanced stages of some tumors with a marked inflammatory component, such as breast [11, 12], head [13], and neck cancer [13, 14], renal cell carcinoma [15, 16], ovarian cancer [17, 18] and multiple myeloma [6]. For such a reason, COX-1 could be considered a biomarker for the early detection of tumors.

*Address correspondence to these authors at the Department of Pharmacy-Pharmaceutical Sciences, University of Bari, Italy; Tel: +39 0805442753-47; Fax: +39 0805442724; Mobile +39 3204950508; E-mails: antonio.scilimati@uniba.it; mariagrazia.perrone@uniba.it;

1573-4080/xx $65.00+.00

To investigate COX structure and function relationships, the need for a larger quantity of pure enzyme is essential [19-21]. X-ray crystallography is a useful technique allowing the direct visualization of protein structure at the atomic or near-atomic level applied to a single crystal of pure proteins. Pure protein availability is also fundamental for other functional experiments, such as the oxygen consumption measurement, during the COX-mediated AA bis-oxygenation, since mitochondrial respiration and reactive oxygen species (ROS) can interfere if whole cells are used. The production of a target enzyme is commonly the rate-limiting step, especially for structural studies where the protein yield must be significantly high. For this reason, an efficient production system that not only allows high pure protein yield but also preserves both catalytic activity and quaternary structure is needed. *Escherichia coli (E. coli)* is the workhorse of recombinant protein production due to its rapid growth and ability to efficiently express proteins at very high levels. Indeed, many X-ray crystal structures have been solved on proteins produced by *E. coli*.

Compared to bacteria, the Baculovirus expression system revealed to be a superior methodology for high-level recombinant protein expression due to its capacity to insert foreign target genes of large size and for a strong AcMNPV polyhedrin (PH) promoter, guaranteeing a higher probability of success [22]. Furthermore, the Baculovirus system was chosen for our purpose of being able to provide a variety of co-translational and post-translational modifications of the recombinant proteins such as *N*-glycosylation, which occurs in the endoplasmic reticulum that is crucial for COX-1 folding and function. As a result, insect cell-expressed proteins have biological activities and immunological reactivity comparable to those of proteins expressed in mammalian cells. Among the numerous Baculoviruses, *Autographa californica multiple NPV* (AcMNPV) is the most well-studied and the most expansively applied insect virus [2, 23, 24].

Herein, the development of a simple and efficient protocol for the large-scale expression of recombinant *ovine*COX-1 (*o*COX-1) in a soluble and active form is reported. Besides, an improved purification protocol of *o*COX-1 is described.

2. MATERIAL AND METHODS

2.1. Transformation of pFastBac/*o*COX-1 plasmid in DH10Bac *E. coli* Cells

The recombinant pFastBac/*o*COX-1 plasmid was provided by Prof. M. Malkowski (University of Buffalo, USA). Such a plasmid was sequenced and no mutations were found. The sequence matches the sheep PGHS-1 in the GenBank database (GenBank: J03599.1) [25, 26].

The appropriate amount of recombinant plasmid (30 ng) was transformed into DH10Bac *E. coli* high competent cells (100 µl), used as the host for the pFastBac vector, for transposition into a bacmid. Blue-White screening was performed and white colonies, supposed to contain recombinant clones, were selected and analyzed by PCR, using pUC/M13 forward and reverse primers at a final concentration of 250 nM (Table **1**).

Table 1. pUC/M13 For. and Rev. primers sequences.

Primers	Sequence
pUC/M13 Forward	5′-CCCAGTCACGACGTTGTAAAACG-3′
pUC/M13 Reverse	5′-AGCGGATAACAATTTCACACAGG-3′

PCR was carried out in a final volume of 50 µl, using a proofreading Taq DNA Polymerase (Thermo Fisher Scientific). Thermocycling conditions were 93°C for 180 s, then 30 cycles of 45 s at 94°C, 45 s at 55°C touchdowns and 5 min at 72°C, followed by a final extension of 72°C for 5 min. PCR products were electrophoresed on 1% (w/v) agarose gels and visualized with UV. The PCR reaction products were separated by 1% (w/v) agarose gel electrophoresis and visualized by UV. A single colony, confirmed to have a white phenotype on restreaked plates containing Bluogal, was inoculated in a larger liquid culture (100 ml). Then, once the success of the transposition of the *o*COX-1 gene into bacmid has been confirmed, a slightly modified Promega PureYield Plasmid miniprep system protocol was used to isolate recombinant bacmid DNA. The cell lysis and neutralization were performed following the standard procedure. Then, purification was carried out using isopropanol precipitation and extensive centrifugation at maximum speed in a microcentrifuge for 20 minutes. The DNA pellet was resuspended in 70% ethanol and centrifuged at maximum speed for 5 minutes. The purified pellet was incubated at room temperature (23 - 25 °C) for 10 minutes and then stored in Tris-EDTA buffer at 4°C until use.

2.2. Transfection of Recombinant DNA Bacmid Into Sf9 Insect Cells

Transfection of healthy Sf9 cells with the recombinant DNA bacmid was carried out by using Cellfectin II reagent, a cationic-lipid formulation, designed to ensure an efficient and consistent transfection of insect cells [23]. Briefly, in a 6-well tissue culture plate, Sf9 cells at 95-97 % of viability were seeded at $9x10^5$ per well in 2 ml of Sf-900 II SFM (Gibco) medium without antibiotics and incubated at 28°C for at least 1 hour for cell attachment. When the density of the Sf9 cells reached 75-80%, the recombinant bacmid DNA: Cellfectin complex was kept for 25 minutes at RT and then was overlaid gently from the wall of the well onto the cells and incubated at 28°C in a humidified incubator for 5 hours. After incubation, the medium was replaced with Sf-900 II SFM containing 10 % fetal bovine serum (FBS), 1 % penicillin/streptomycin, and the cells were incubated at 27.5°C for at least 72 hours. Different transfection conditions were tested by varying only the bacmid DNA concentration (Table **2**).

After incubation at 28°C in a humidified incubator for 3-5 hours, the transfection mixture was replaced with the regu-

Table 2. Bacmid DNA tested to generate the recombinant baculovirus.

Transfection Condition	pure Bacmid DNA (µg)	Cellfectin II Reagent (µl)
1	0.5	8
2	1	8
3	2	8
4	3	8
5	6	8

lar culture medium containing 10% no-deactivated FBS and 1% penicillin/streptomycin antibiotics. Evident signs of a viral infection such as increased cell diameter, granular appearance, and detachment were observed after 3 days by using conditions 3 and 4; in all other conditions, the transfection was successful only after 6 days (data not shown). From all conditions tested, the supernatant was harvested and the low titer P0 viral stock was obtained. Then, P0 was amplified twice, to afford the higher titer baculoviral stock P2, optimal to carry out recombinant protein expression. The P2 baculoviral titer was determined by viral plaque and it was found to be ~$5x10^8$ pfu/ml.

2.3. 8xHis-tag/*o*COX-1 Expression

A fresh and viable Sf9 insect cell suspension at a cell density of 2-$2.5x10^6$ cells/ml was infected with baculoviral stock P2 (~$5x10^8$ pfu/ml) to express the *N*-terminal His-tagged *o*COX-1 recombinant protein.

After 72 hours of incubation at 28°C, cells were harvested by centrifugation at 900xg for 20 minutes at 4°C. The cell pellet was rapidly cooled in liquid nitrogen and immediately stored at -80°C until needed. Such conditions were used to avoid protein degradation until the purification step.

2.4. Recombinant *o*COX-1 Purification

Cell pellet from 1 L culture was resuspended in Lysis buffer [30 ml, 20 mM Tris-HCl pH 8.0, 100 mM KCl, 10 µl/ml complete EDTA-free protease inhibitor, 10 µl/ml PMSF] and disrupted by French Press. *o*COX-1 was then solubilized from the membranes by adding 0.8% w/v $C_{10}E_6$ (*Hexaethylene Glycol Monodecyl Ether, Anatrace)* with gentle agitation for at least 2 hours at 4 °C. The insoluble fractions was removed at 100,000xg for 1 hour. After centrifugation, the supernatant was carefully removed and rapidly purified by Immobilized Metal Affinity Chromatography (IMAC). Specifically, one milliliter of Ni^{2+}-NTA low density agarose beads (GoldBio) was pre-equilibrated with *Ni*-Buffer [20 mM Tris-HCl pH 8.0, 100 mM KCl, 5 mM imidazole, 0.1% $C_{10}E_6$, 5% glycerol], and then rotated for 3 hours at 4 °C with the supernatant. The mixture was poured into a column and the flow-through (FT) was collected. The column was, then, washed with 250 ml of Wash Buffer I [20 mM Tris-HCl pH 8.0, 0.5 M KCl, 10 mM imidazole, 0.1% $C_{10}E_6$ and 5% glycerol], followed by 250 ml of Wash Buffer II [20 mM Tris-HCl pH 8.0, 40 mM KCl, 20 mM imidazole, 0.1% $C_{10}E_6$ and 5% glycerol].

Bound octahistidine-tagged *o*COX-1 was eluted with buffer containing 150 mM imidazole [20 mM Tris-HCl pH 8.0, 40 mM KCl, 150 mM imidazole, 0.1% $C_{10}E_6$ and 5% glycerol]. Each fraction was incubated for 5 minutes at before collection. The polyhistidine tail was removed from the recombinant protein using Tobacco Etch Virus (TEV) in a ratio of 1:40 w/w protease to protein for 12-16 hours at 4°C, and a second IMAC chromatography (0.5 ml Ni^{2+}-NTA resin) was performed. The FT containing the untagged protein was collected. Buffer exchange was also performed to lower imidazole concentration to a final concentration of 5 mM. Fractions containing the purified *o*COX-1 protein were pooled and quantified using BCA protein assay (Pierce). The final yield obtained was 1 mg of pure protein starting from 1 L of infected Sf9 cells.

2.5. Cyclooxygenase Activity Assay by O_2 Electrode

The monitoring of COX activity was accomplished by measuring O_2 consumption with the Oxytherm electrode unit (Hansatech). This method uses a Clark-type oxygen electrode to monitor over time the dissolved oxygen concentration in a sealed chamber. Oxygen consumption was measured at 37°C directly in a 1000 µL reaction vessel. A typical assay: oxygraph buffer (the opportune volume is adjusted to 1000 µL of the final volume in accordance to the volume of the enzyme), 5 µM hemin (2 µL), 100 µM arachidonic acid (20 µL), and either inhibitor (10 µL), in this case, mofezolac, a selective COX-1 inhibitor, at the opportune concentrations (0.1, 1, 10, 50, 100, 500 µM) or vehicle (DMSO). Oxygen consumption determination starts after the addition of enzyme (1.3 mg/mL).

3. RESULTS AND DISCUSSION

The expression and purification of recombinant *o*COX-1 protein using the Baculovirus expression system were accomplished approximately a decade ago to carry out biochemical and structural investigations aimed at identifying the molecular architecture of the COX homodimer [27]. In the present study, the pFastBac vector was confirmed to be the suitable target gene transfer vector and the recombinant *o*COX-1 protein was efficiently produced by the Bac-to-Bac Baculovirus Expression system.

Firstly, the pFastbac donor construct was sequenced and then used to transform *E. coli* high competent cells. The blue/white selection was carried out to identify colonies containing the recombinant bacmid. The presence of the *o*COX-1 gene in the recombinant bacmid was evaluated by PCR analysis. pUC/M13 forward and reverse primers (Table **1**) were used to amplify the bacmid DNA from a white colony, and a PCR product of the expected size (~4966 bp) was obtained. The amplified bacmid DNA PCR product was visualized by on 1% agarose gel electrophoresis (Fig. **1**), which indicated that the insert was successfully transposed in the bacmid DNA (Lane 3).

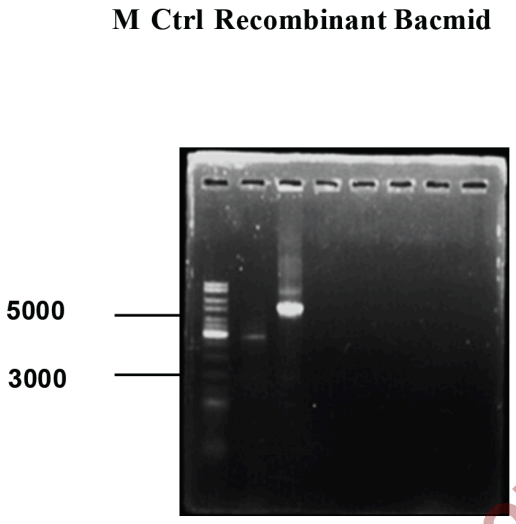

Fig. (1). Agarose gel electrophoresis of bacmid DNA PCR product directly from the plate. **Lane 1**, Gene Ruler DNA Ladder; **Lane 2**, pUC19 (2686 bp), as a control for transformation; **Lane 3**, PCR product of recombinant bacmid DNA amplified with pUC/M13 reverse primers. The expected PCR product with higher size was obtained (2300 bp + 2666 bp *o*COX-1 gene) from the picked white colony, demonstrating the presence of the gene of interest in the recombinant bacmid. *(A higher resolution / colour version of this figure is available in the electronic copy of the article)*

This result encouraged us to produce a greater quantity of the recombinant bacmid. The recombinant baculovirus was then generated following transfection in Sf9 cells, which show evident features of infection such as increased cell diameter, detachment, and cell lysis. These characteristics supported the successful construction of the recombinant baculovirus. A small suspension of Sf9 cells was infected by recombinant baculovirus and Western blot analysis was performed, using an anti-COX-1 mouse monoclonal antibody (1:500, overnight at 4 °C; COX-111, Invitrogen). WB results revealed a strong protein band in lane 2 with respect to the control HEK-293 COX-1 (Fig. **2**). Engineered cell line HEK-293 COX-1 expressing COX-1, and not COX-2, upon stimulation with 10 µg/mL tetracycline, was used as a positive control.

Several limits of the known procedure [2] were encountered mainly in the expression step, such as the low production yield of the recombinant protein due to its tendency to

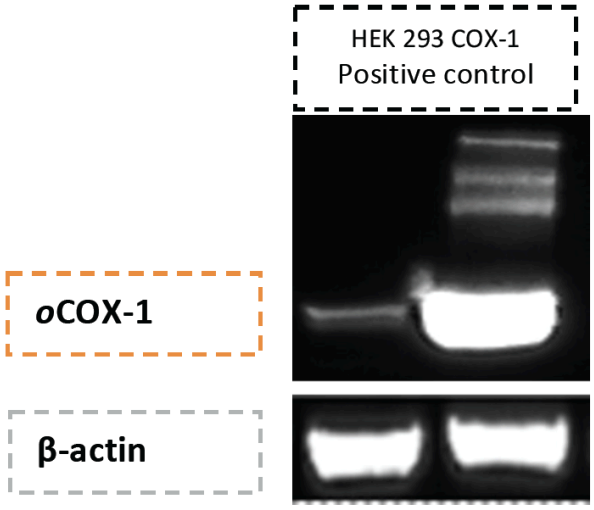

Fig. (2). Western blot analysis of *o*COX-1 expression in Sf9 cells infected with the recombinant baculovirus. **Lane 1**: HEK-293 COX-1 positive control; **Lane 2**: infected Sf9 cell lysate. β -actin level was used as the loading control. *(A higher resolution / colour version of this figure is available in the electronic copy of the article).*

form aggregates. Refolding recombinant proteins from insoluble aggregates often results in low yields of correctly folded proteins. To overcome such a limit, a proper approach aimed at increasing the yield of the purified recombinant protein was developed by us.

Specifically, some parameters were optimized. First, the volume of the suspension culture was lowered to 1 L increasing the cell density up to 2-2.5x10^6 cells/ml instead of 1x10^6 cells/ml, and with 97% cell viability. Consequently, a higher yield in the production of the protein was observed purifying 1 L at once instead of 5 L starting volume. For protein overexpression, the multiplicity of infection (M.O.I.) was also increased from 0.1 up to 10, to get all the cells infected and synchronously. As a result, about 100 % infection rate was reached.

Besides, although it is reported that the maximum expression of non-secreted proteins is observed up to 96 hours post-infection [23], in our hands 72 hours post-infection was found to be optimal. By performing a time course of the infection, a good infection level was reached between 48 and 72 hours after the inoculation of the high titer baculoviral stock (data not shown). Prolonging the infection after 72 hours, protein degradation by cellular proteases or by cellular content released in the medium may occur, with consequent loss of protein.

A crucial point in the purification of *o*COX-1 is its recovery which has been increased by detaching the protein from the endoplasmic reticulum membrane using the non-ionic and non-denaturing detergent $C_{10}E_6$ at a final concentration of 0.8% w/v [2]. Rising incubation time of the cell lysate with the detergent to at least 2 hours, a larger amount of protein was isolated from the membrane determining an increase of the protein solubility, still preserving the correct folding and the enzymatic catalytic activity as determined by

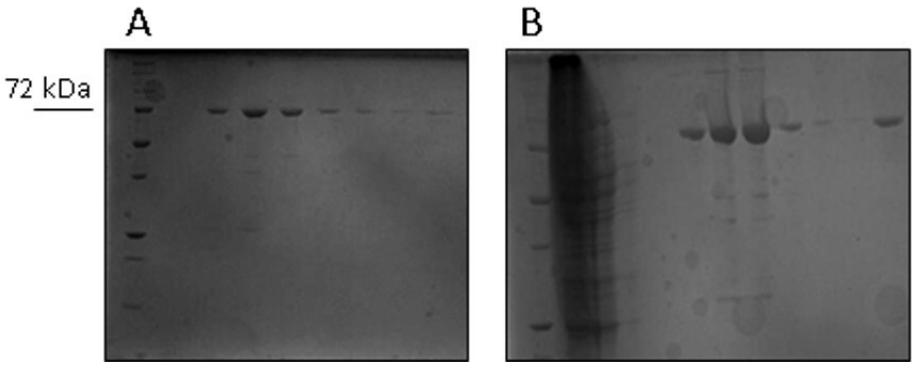

Fig. (3). SDS PAGE profile from the purification phase. **(A)** SDS-PAGE analysis of the eluted fractions after the first incubation (3 hours). **Lane 1**: marker; **Lane 2**: washing buffer at low salt concentration; **Lane 3-8**: fractions collected by 150 mM imidazole buffer; **Lane 9**: Ni^{2+}-NTA agarose beads. **(B)** SDS-PAGE analysis of the eluted fractions after 12 hours of FT re-incubation. **Lane 1**: marker; **Lane 2**: flow-through; **Lane 3**: washing buffer at high salt concentration; **Lane 4**: washing buffer at low salt concentration; **Lane 5-10**: fractions collected by 150 mM imidazole buffer. *(A higher resolution / colour version of this figure is available in the electronic copy of the article).*

Cyclooxygenase O_2 Electrode Assay [28, 29]. The insoluble (pellet) and the soluble fractions (supernatant) were separated at 100,000xg for 1 hour instead of 2 hours. The supernatant containing the recombinant protein was then subjected to immobilized metal affinity chromatography (IMAC). Ni^{2+}-NTA was used as a ligand chelator because the recombinant *o*COX-1 included an amino acid motif consisting of 8 residues fused to its *N*-terminal portion.

The optimization of the purification step significantly contributed to the protein production yield: in the initial experiments, the solubilized protein was incubated for 3 hours in the presence of Ni^{2+}-NTA agarose resin. The tagged *o*COX-1 was then eluted from the column using increasing imidazole concentrations. To improve the purification efficiency, the FT was subjected to a further chromatography step by re-incubating it with the Ni^{2+}-NTA resin for 12 hours at 4 °C. The largest amount of pure protein in the elution fractions was obtained after 12 hours of incubation.

Protein samples from the purification step were separated by 12% SDS-PAGE gels (Fig. **3**). The gels were stained with Blue Coomassie and the protein was identified by comparing the *o*COX-1 protein band to the molecular weight marker (Precision Plus Protein™ Dual Color Standards, Bio-Rad). It is noteworthy that FT incubation for 12 hours affords the highest yield of protein in the eluted fractions. Furthermore, SDS-PAGE analysis of selected fractions has shown that the eluted protein is highly pure, so avoiding the need for further purification steps as no low molecular weight species are detectable after Blue Coomassie staining the gel (Fig. **3A** and **3B**). The above-described modifications have useful for the efficient purification and isolation of the recombinant *o*COX-1, which are of fundamental importance for the characterization of its function and structure. Western blotting analysis of the eluted fractions was also performed (Fig. **4**).

The Ni^{2+}-NTA strategy takes advantage of a small peptide sequence of 8 Histidine residues fused to the N-terminal domain of recombinant *o*COX-1 to easily detect and purify the expressed protein. However, the presence of the tag in the purified protein could contribute to the overall flexibility of the whole protein or its terminus, thus disturbing the structural analysis. Additionally, the tag can negatively affect protein-ligand interactions, such as in drug-COX inhibitors screenings. Therefore, it is advisable to remove the tag by using a suitable protease. Our recombinant protein contains a TEV protease site located at the *N*- terminus of the protein, downstream of the 8xHis sequence [25, 30].

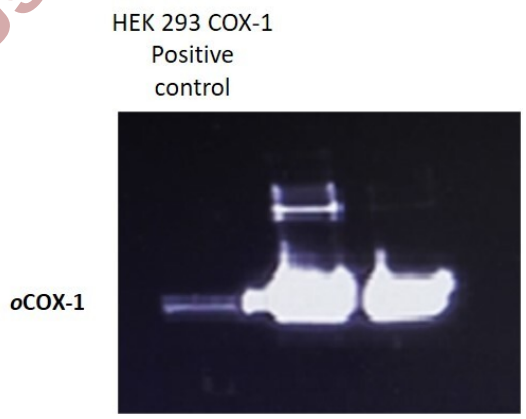

Fig. (4). Western blot analysis of *o*COX-1 eluted from the Nickel-NTA column. **Lane 1**: HEK-293 COX-1 positive control; **Lane 2-3**: eluted fractions. *(A higher resolution / colour version of this figure is available in the electronic copy of the article).*

The 8xHis sequence cleavage was directly performed on the eluted fraction for 12-16 hours at 4 °C, without changing the buffer or concentrating the protein by ultrafiltration. The digestion mixture was then loaded on the affinity column and purified by IMAC (*Recapture on Beads*). Under these conditions, the untagged-*o*COX-1 protein is unable to bind to the nickel on the beads, and hence the protein is eluted from the column. After the *Recapture on Beads* step, almost 90% of the recombinant protein was recovered in the flow-through, indicating that the cleavage of the Histidine tail was highly efficient (Fig. **5**).

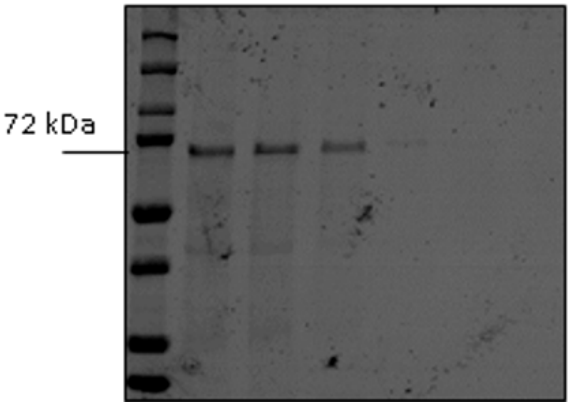

Fig. (5). SDS PAGE profile from the cleavage step. **Lane 1**: marker; **Lane 2**: undigested/sample control; **Lane 3**: flow-through; **Lane 4**: washing buffer at low salt concentration, without imidazole; **Lane 5-7**: fractions collected by 150 mM imidazole buffer. *(A higher resolution / colour version of this figure is available in the electronic copy of the article)*

The pure untagged-*o*COX-1 was then collected and quantified using BCA protein assay (Pierce). A higher yield was observed when the pellet from 1 L at a time was processed and purified instead of pellet deriving from bigger volumes of cells infected such as 2 L or 4 L (Table **3**).

The enzymatic activity of the purified *o*COX-1 has been determined with cyclooxygenase O_2 electrode assay by using the oxygraph. By inhibiting COX-1, the amount of oxygen necessary to AA bis-oxygenation was reduced. In presence of increasing mofezolac concentrations mofezolac concentration, a selective COX-1 inhibitor, a reduction in the O_2 consumption was observed, indicating that the purified enzyme was properly folded and still active (Fig. **6**), and its specific activity is 40,000 unit/mg ± 0.49.

CONCLUSION

In conclusion, we described the improvements of a previously reported method for pure recombinant *o*COX-1 production and isolation [23]. In summary, we (a) lowered the starting volume of infected cells for each purification, (b) increased the cell density and the number of viral particles per cell, and (c) shortened the infection period. Concerning the purification, the protein solubilization time in the presence of a non-ionic detergent was prolonged and a second purification step by re-applying the first IMAC flow-through to the nickel resin was introduced. This optimized procedure could be suited also to produce other membrane proteins, for which an improvement in the solubilizing step is needed to protein at high concentration. Future work should be aimed at gaining the deepest insights into the inhibitor-enzyme interactions to better develop compounds endowed with nanomolar activity towards COX-1 useful for theragnostic agent design.

Table 3. Protein obtained starting from different volumes of Sf9 infected cells.

Cells infected (L)	Pure *o*COX-1 (mg)
4 L total 1 L at a time processed	4.0 mg
4 L total 2 L at a time processed	3.09 mg
8 L total 4 L at a time processed	4.36 mg

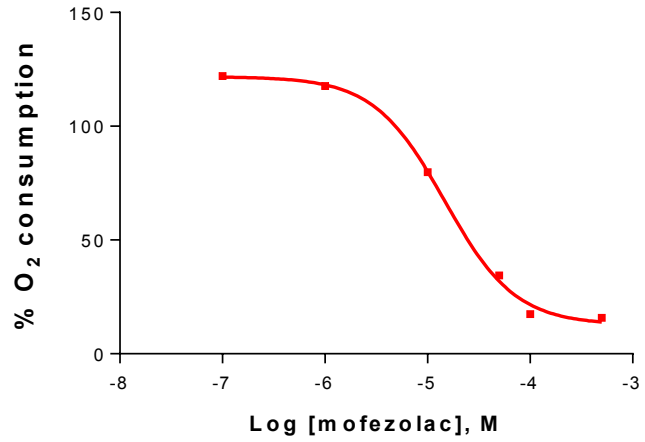

Fig. (6). *Cyclooxygenase O_2 Electrode Assay*. O_2 consumption by the purified *ovine*COX-1 decreases (%) in the presence of increasing mofezolac concentrations.

AUTHORS' CONTRIBUTIONS

Morena Miciaccia and Mariaclara Iaselli contributed equally to this work.

ETHICS APPROVAL AND CONSENT TO PARTICIPATE

Not applicable.

HUMAN AND ANIMAL RIGHTS

The authors declare no conflict of interest, financial or otherwise.

CONSENT FOR PUBLICATION

Not applicable.

AVAILABILITY OF DATA AND MATERIALS

The data used to support the findings of this study are available from the corresponding author upon request.

FUNDING

This work was supported by Associazione Italiana per la Ricerca sul Cancro (AIRC), MFAG2015 (Project Id. 17566), Associazione Progetto G.A.I.A.

CONFLICT OF INTEREST

The authors declare no conflict of interest, financial or otherwise.

ACKNOWLEDGEMENTS

We thank Prof. Gino Cingolani of Thomas Jefferson University (Philadelphia-USA) for the helpful suggestions and guesting MM and MI into his laboratory to carry out part of the work herein described.

REFERENCES

[1] Smith, W.L.; Garavito, R.M.; DeWitt, D.L. Prostaglandin endoperoxide H synthases (cyclooxygenases)-1 and -2. *J. Biol. Chem.,* **1996**, *271*(52), 33157-33160. http://dx.doi.org/10.1074/jbc.271.52.33157 PMID: 8969167

[2] Sidhu, R.S.; Lee, J.Y.; Yuan, C.; Smith, W.L. Comparison of cyclooxygenase-1 crystal structures: cross-talk between monomers comprising cyclooxygenase-1 homodimers. *Biochemistry,* **2010**, *49*(33), 7069-7079. http://dx.doi.org/10.1021/bi1003298 PMID: 20669977

[3] Smith, W.L.; Malkowski, M.G. Interactions of fatty acids, nonsteroidal anti-inflammatory drugs, and coxibs with the catalytic and allosteric subunits of cyclooxygenases-1 and -2. *J. Biol. Chem.,* **2019**, *294*(5), 1697-1705. http://dx.doi.org/10.1074/jbc.TM118.006295 PMID: 30710016

[4] Dong, L.; Sharma, N.P.; Jurban, B.J.; Smith, W.L. Pre-existent asymmetry in the human cyclooxygenase-2 sequence homodimer. *J. Biol. Chem.,* **2013**, *288*(40), 28641-28655. http://dx.doi.org/10.1074/jbc.M113.505503 PMID: 23955344

[5] Vitale, P.; Panella, A.; Scilimati, A.; Perrone, M.G. COX-1 Inhibitors: Beyond Structure Toward Therapy. *Med. Res. Rev.,* **2016**, *36*(4), 641-671. http://dx.doi.org/10.1002/med.21389 PMID: 27111555

[6] Pati, M.L.; Vitale, P.; Ferorelli, S.; Iaselli, M.; Miciaccia, M.; Boccarelli, A.; Di Mauro, G.D.; Fortuna, C.G.; Souza Domingos, T.F.; Rodrigues Pereira da Silva, L.C.; de Pádula, M.; Cabral, L.M.; Sathler, P.C.; Vacca, A.; Scilimati, A.; Perrone, M.G. Translational impact of novel widely pharmacological characterized mofezolac-derived COX-1 inhibitors combined with bortezomib on human multiple myeloma cell lines viability. *Eur. J. Med. Chem.,* **2019**, *164*, 59-76. http://dx.doi.org/10.1016/j.ejmech.2018.12.029 PMID: 30590258

[7] Casalino, G.; Coluccia, M.; Pati, M.L.; Pannunzio, A.; Vacca, A.; Scilimati, A.; Perrone, M.G. Intelligent microarray data analysis through nonnegative matrix factorization to study human multiple myeloma cell lines. *Appl. Sci. (Basel),* **2019**, 9(24), 5552. http://dx.doi.org/10.3390/app9245552

[8] Herschman, H.R. Prostaglandin synthase 2. *Biochim. Biophys. Acta,* **1996**, *1299*(1), 125-140. http://dx.doi.org/10.1016/0005-2760(95)00194-8 PMID: 8555245

[9] Ricciotti, E.; FitzGerald, G.A. Prostaglandins and inflammation. *Arterioscler. Thromb. Vasc. Biol.,* **2011**, *31*(5), 986-1000. http://dx.doi.org/10.1161/ATVBAHA.110.207449 PMID: 21508345

[10] Perrone, M.G.; Lofrumento, D.D.; Vitale, P.; De Nuccio, F.; La Pesa, V.; Panella, A.; Calvello, R.; Cianciulli, A.; Panaro, M.A.; Scilimati, A. Selective cyclooxygenase-1 inhibition by p6 and gastrotoxicity: preliminary investigation. *Pharmacology,* **2015**, *95*(1-2), 22-28. http://dx.doi.org/10.1159/000369826 PMID: 25591798

[11] Kennedy, B.M.; Harris, R.E. Cyclooxygenase and lipoxygenase gene expression in the inflammogenesis of breast cancer. *Inflammopharmacology,* **2018**, *26*, 909-923. http://dx.doi.org/10.1007/s10787-018-0489-6 PMID: 29736687

[12] Wyatt, G.L.; Crump, L.S.; Young, C.M.; Wessells, V.M.; McQueen, C.M.; Wall, S.W.; Gustafson, T.L.; Fan, Y.Y.; Chapkin, R.S.; Porter, W.W.; Lyons, T.R. Cross-talk between SIM2s and NFκB regulates cyclooxygenase 2 expression in breast cancer. *Breast Cancer Res.,* **2019**, *21*(1), 131-143. http://dx.doi.org/10.1186/s13058-019-1224-y PMID: 31783895

[13] Frejborg, E.; Salo, T.; Salem, A. Role of cyclooxygenase-2 in head and neck tumorigenesis. *Int. J. Mol. Sci.,* **2020**, *21*(23), 9246-9263. http://dx.doi.org/10.3390/ijms21239246 PMID: 33287464

[14] Lipari, L.; Mauro, A.; Gallina, S.; Tortorici, S.; Buscemi, M.; Tete, S.; Gerbino, A. Expression of gelatinases (MMP-2, MMP-9) and cyclooxygenases (COX-1, COX-2) in some benign salivary gland tumors. *Int. J. Immunopathol. Pharmacol.,* **2012**, *25*(1), 107-115. http://dx.doi.org/10.1177/039463201202500113 PMID: 22507323

[15] Osman, W.M.; Youssef, N.S. Combined use of COX-1 and VEGF immunohistochemistry refines the histopathologic prognosis of renal cell carcinoma. *Int. J. Clin. Exp. Pathol.,* **2015**, *8*(7), 8165-8177. PMID: 26339385

[16] Yu, Z.H.; Zhang, Q.; Wang, Y.D.; Chen, J.; Jiang, Z.M.; Shi, M.; Guo, X.; Qin, J.; Cui, G.H.; Cai, Z.M.; Gui, Y.T.; Lai, Y.Q. Overexpression of cyclooxygenase-1 correlates with poor prognosis in renal cell carcinoma. *Asian Pac. J. Cancer Prev.,* **2013**, *14*(6), 3729-3734. http://dx.doi.org/10.7314/APJCP.2013.14.6.3729 PMID: 23886173

[17] Perrone, M.G.; Luisi, O.; De Grassi, A.; Ferorelli, S.; Cormio, G.; Scilimati, A. Translational theragnosis of ovarian cancer: where do we stand? *Curr. Med. Chem.,* **2020**, *27*(34), 5675-5715. http://dx.doi.org/10.2174/0929867326666190816232330 PMID: 31419925

[18] Malerba, P.; Crews, B.C.; Ghebreselasie, K.; Daniel, C.K.; Jashim, E.; Aleem, A.M.; Salam, R.A.; Marnett, L.J.; Uddin, M.J. Targeted detection of cyclooxygenase-1 in ovarian cancer. *ACS Med. Chem. Lett.,* **2019**, *11*(10), 1837-1842. http://dx.doi.org/10.1021/acsmedchemlett.9b00280 PMID: 33062161

[19] Rouzer, C.A.; Marnett, L.J. Cyclooxygenases: Structural and functional insights. *J. Lipid. Res. Suppl.,* **2009**, *50*, 29-34.

[20] Gupta, K.; Selinsky, B.S.; Kaub, C.J.; Katz, A.K.; Loll, P.J. The 2.0 A resolution crystal structure of prostaglandin H2 synthase-1: Structural insights into an unusual peroxidase. *J. Mol. Biol.,* **2004**, *335*(2), 503-518. http://dx.doi.org/10.1016/j.jmb.2003.10.073 PMID: 14672659

[21] Smith, T.; Leipprandt, J.; DeWitt, D. Purification and characterization of the human recombinant histidine-tagged prostaglandin endoperoxide H synthases-1 and -2. *Arch. Biochem. Biophys.,* **2000**, *375*(1), 195-200. http://dx.doi.org/10.1006/abbi.1999.1659 PMID: 10683267

[22] Nettleship, J.E.; Assenberg, R.; Diprose, J.M.; Rahman-Huq, N.; Owens, R.J. Recent advances in the production of proteins in insect and mammalian cells for structural biology. *J. Struct. Biol.,* **2010**, *172*(1), 55-65. http://dx.doi.org/10.1016/j.jsb.2010.02.006 PMID: 20153433

[23] Bac-to-Bac® Baculovirus Expression System, Invitrogen. **1994**.

[24] Barnett, J.; Chow, J.; Ives, D.; Chiou, M.; Mackenzie, R.; Osen, E.; Nguyen, B.; Tsing, S.; Bach, C.; Freire, J.; Chana, H.; Sigalb, E.; Rameshab, C. Purification, characterization and selective inhibition of human prostaglandin G/H synthase 1 and 2 expressed in the baculovirus system. *Biochim. Biophys. Acta,* **1994**, *1209*(1), 130-139. http://dx.doi.org/10.1016/0167-4838(94)90148-1 PMID: 7947975

[25] DeWitt, D.L.; Smith, W.L. Primary structure of prostaglandin G/H synthase from sheep vesicular gland determined from the complementary DNA sequence. *Proc. Natl. Acad. Sci. USA,* **1988**, *85*(5), 1412-1416. http://dx.doi.org/10.1073/pnas.85.5.1412 PMID: 3125548

[26] Thuresson, E.D.; Lakkides, K.M.; Rieke, C.J.; Sun, Y.; Wingerd, B.A.; Micielli, R.; Mulichak, A.M.; Malkowski, M.G.; Garavito, R.M.; Smith, W.L. Prostaglandin endoperoxide H synthase-1: The functions of cyclooxygenase active site residues in the binding, positioning, and oxygenation of arachidonic acid. *J. Biol. Chem.,* **2001**, *276*(13), 10347-10357. http://dx.doi.org/10.1074/jbc.M009377200 PMID: 11121412

[27] Perrone, M.G.; Miciaccia, M.; Vitale, P.; Ferorelli, S.; Araújo, C.D.C.B.; de Almeida, G.S.; Souza Domingos, T.F.; da Silva, L.C.R.P.; de Pádula, M.; Cabral, L.M.; Sathler, P.C.; Bonaccorso, C.; Fortuna, C.G.; Scilimati, A. An attempt to chemically state the cross-talk between monomers of COX homodimers by double/hybrid inhibitors mofezolac-spacer-mofezolac and mofezolac-spacer-arachidonic acid. *Eur. J. Med. Chem.,* **2021**, *209*, 112919. http://dx.doi.org/10.1016/j.ejmech.2020.112919 PMID: 33129592

[28] Diepart, C.; Verrax, J.; Calderon, P.B.; Feron, O.; Jordan, B.F.; Gallez, B. Comparison of methods for measuring oxygen consumption in tumor cells *in vitro*. *Anal. Biochem.,* **2010**, *396*(2), 250-256. http://dx.doi.org/10.1016/j.ab.2009.09.029 PMID: 19766582

[29] Mbonye, U.R.; Wada, M.; Rieke, C.J.; Tang, H-Y.; Dewitt, D.L.; Smith, W.L. The 19-amino acid cassette of cyclooxygenase-2 mediates entry of the protein into the endoplasmic reticulum-associated degradation system. *J. Biol. Chem.,* **2006**, *281*(47), 35770-35778. http://dx.doi.org/10.1074/jbc.M608281200 PMID: 17001073

[30] Koksal, A.C.; Nardozzi, J.D.; Cingolani, G. Dimeric quaternary structure of the prototypical dual specificity phosphatase VH1. *J. Biol. Chem.,* **2009**, *284*(15), 10129-10137. http://dx.doi.org/10.1074/jbc.M808362200 PMID: 19211553